

1 **6 February 2026**

2 **JAB_2025-0337.R1**

3 **Ear-worn inertial sensors can predict gait metrics**
4 **and reconstruct vertical ground reaction force curves during running**

5

6 Jake Stuchbury-Wass¹, Mathias Ciliberto¹, Kayla-Jade Butkow¹, Qiang Yang¹, Yang Liu¹,
7 Ezio Preatoni², Dong Ma³ and Cecilia Mascolo¹

8 ¹Department of Computer Science and Technology, University of Cambridge, UK

9 ²Department for Health, University of Bath, UK

10 ³School of Computing and Information Systems, Singapore Management University

11

12 **Conflict of Interest Disclosure:** None to declare.

13

14 **Correspondence Address:**

15 Jake Stuchbury-Wass

16 15 JJ Thomson Avenue

17 Cambridge

18 CB3 0FD

19 UK

20

21

22

Abstract

23 Ear-worn wearables (aka: earbuds, hearables, or earables) are commonly used by runners for
24 entertainment, and many modern devices also include inertial sensors for user interaction. We
25 propose harnessing the technology embedded in earbuds to capture fundamental aspects of
26 running mechanics and make them available to the wider community of users, outside a lab
27 setting. While other wearables such as insoles, or ankle/sacrum mounted IMUs have already
28 been presented, ear-worn devices may have a better potential for adoption and therefore offer
29 an optimal compromise between validity of running gait analysis and usability. Thirty healthy
30 participants (18 male, 12 female) ran on an instrumented treadmill (54000 gait cycles) and
31 floor-mounted force plates (2800 gait cycles) at a variety of speeds. Building on the information
32 brought about by the vibrations transmitted to, and motion of the head, we devised a gait event
33 detection algorithm and a regression model to predict vertical ground reaction force (vGRF)
34 waveforms. The validation of outcomes against quantities from force plates shows an average
35 MAPE of 4.8 % on temporal metrics and 9.0 % on scalar GRF derived metrics. Additionally,
36 the model tracks the full vGRF curve well, achieving an NRMSE of 11.1 % on unseen
37 participants. Overall, we show comparable accuracy from an ear-worn consumer device in
38 temporal and kinetic gait parameter estimation to specialist devices, paving the way for
39 accessible running gait monitoring.

40

41 ***Keywords:* Running gait, kinetics, motion capture, machine learning, wearables**

42

Introduction

43 Running is one of the most popular sporting activities worldwide, with an estimated
44 621 million people participating globally [13]. During running, measuring gait events and
45 ground reaction forces are essential for supporting performance analysis and injury prevention
46 [5]. Direct links to injuries such as tibial stress fractures from ground reaction forces are
47 debated in the literature e.g. [22], however, ground reaction forces are necessary to derive
48 downstream measures, such as joint loading and moments, which have been indicated as
49 biomechanical factors associated with injury risk [5]. Measurements of gait and ground
50 reaction force metrics are typically confined to motion capture laboratories equipped with
51 specialised equipment such as force plates, instrumented walkways, treadmills, and systems
52 for kinematic analysis. Laboratory-based testing is costly, requires trained personnel, and
53 provides only a limited, non-continuous snapshot of an individual's behaviour. Wearable
54 technologies have emerged as a promising alternative for in-field gait analysis. However, to be
55 truly effective and trusted, these devices must undergo rigorous validation [26].

56 Research aimed at predicting running gait events or ground reaction forces (GRF) via
57 wearables emerged with works using the motion markers in a rigid body model to approximate
58 gait kinetics [3] or how parameters of mass-spring model may be optimised to better capture
59 movement kinetics [9]. Modern approaches typically employ pressure insoles e.g. [4] or inertial
60 measurement units (IMUs) mounted on single locations (e.g., sacrum, tibia, foot) e.g. [1, 24]
61 or multiple locations [11, 18, 27]. These studies have utilised dynamical models [24], signal
62 processing-based approaches such as the Kalman filter [20] as well as machine learning
63 approaches including traditional regression models e.g. [27] or deep learning methods such as
64 CNNs [18], RNNs [1], LSTMs [4] and Transformers [34].. There are existing consumer devices
65 that show demand from runners for tracking gait parameters and loading, examples include the
66 Garmin Running Dynamics Pod and some Garmin heart rate monitors (Garmin Ltd., KS, USA)

67 which track a selection of spatiotemporal gait metrics, additionally, Arion Pro (ATO-Gear BV,
68 Eindhoven, Netherlands), NURVV Run (NURVV Ltd., London, UK) and Striv (Striv, MA,
69 USA) smart insoles can track loading using force-sensitive resistors and gait parameters with
70 IMUs. However, all these solutions rely on purpose-built devices that lack widespread adoption
71 or acceptance amongst runners [8]. It has also been demonstrated that ubiquitous smartwatches
72 suffer from large motion artefacts during walking gait assessment [19], and this issue is likely
73 to be exacerbated during running, limiting the suitability for in-depth biomechanical analysis.

74 Ear-worn wearables—commonly referred to as earbuds, hearables, or earables—
75 represent a valuable resource for capturing and monitoring gait information whilst running.
76 They are positioned in a relatively stable location on the body and are owned and regularly
77 used by a majority of runners, with a survey reporting that 72% of runners listen to media
78 whilst running [14]. Modern consumer-market devices, such as Apple AirPods Pro (Apple Inc.,
79 Cupertino, CA, USA), already incorporate inertial sensors for user interactions, such as
80 recognising taps for playing and pausing audio and spatial audio. Consumer-market smart
81 earbuds are currently utilised for spatial audio and actions such as pausing music. Earables
82 could also address challenges in user feedback from wearables by enabling direct audio
83 communication with users rather than relying on screens or vibration [33].

84 Ear-worn transducers are located at the body part farthest from the point of application
85 of ground reaction forces, which might appear counterintuitive to how they can be used to
86 estimate GRFs. However, these transducers receive vibrations generated by foot impact that
87 propagate through the body, and their movement can provide insights into overall centre of
88 mass kinematics. Foot-to-centre-of-mass motion is often modelled using a damped mass-spring
89 system [7, 9, 20, 24]; this could be extended to include the head with an additional damped
90 mass-spring component in the absence of independent head rotations. A machine learning
91 model may be capable of learning these dynamics in this more complex scenario, as

92 demonstrated with foot-to-centre-of-mass relationships e.g. in [1, 34] for the torso and legs
93 predicting vGRFs. We also experimentally observe strong correlations in signal morphology
94 from the head IMU to both sacrum IMU and GRFs showing clear links between the signals.

95 Therefore, we propose using ear-worn wearables, or earables, to monitor gait
96 information whilst running. Whilst related research exists on using earables for gait tracking,
97 the majority of studies focus on walking and clinical applications. For example, Jarchi et al.
98 demonstrated detection of gait events for tracking temporal gait parameters such as cadence
99 and double and single support times during walking [16]. This work was further developed in
100 subsequent research that improved the signal processing algorithm, achieving better accuracy
101 [10, 29]. Later, Atallah et al. also correlated vGRF peak force to ear-worn acceleration peaks;
102 however, R^2 values were approximately 0.3 [2] for mixed user data, and error reporting was
103 not included. A recent study, WalkEar [31], demonstrated how earables can estimate temporal
104 and vGRF parameters during walking with improved correlation results of 0.6-0.9 compared
105 to prior work and reported accuracies comparable to other inertial wearables. This research
106 shows that earables have promise for ground reaction force monitoring, but currently no
107 research on earables for running analysis is available in the literature.

108 We developed and validated a novel algorithm that represents the first to use IMU
109 signals from earables (i.e., the open-source OpenEarable [28]) to enable biomechanical
110 assessment of running. Specifically, we estimate running gait events (e.g., cadence, flight and
111 stance times) and predict individual vertical ground reaction force waveforms and their scalar
112 features (e.g., peak force, loading rate). We devised a new signal processing algorithm and a
113 machine learning regression model with the objective of achieving performance similar to
114 devices worn on the ankle or sacrum while being in a commonly owned form-factor.

115

116

Methods

117 Thirty healthy participants (18 male, 12 female) took part in the study, which was
118 approved by the University of Cambridge Department of Computer Science and Technology
119 ethics committee under application #2134. All participants signed informed consent forms
120 before participating in any experiments and had to be free from current injury as part of the
121 inclusion criteria. The overall demographics and anthropometrics (mean \pm standard deviation)
122 of the participants were an age of 28.2 ± 9.2 years, height of 176.2 ± 8.8 cm and mass of 73.8
123 ± 13.2 kg. Each participant wore their own trainers, sports clothing, and a pair of open-source
124 OpenEarable v1.4 [28], with firmware customised for this project to enable the 50 Hz sampling
125 rate. The newer OpenEarable v2.0 includes this feature in the base firmware among other
126 improvements so our firmware is not available publicly. Each device weighed 12 g and
127 contained a Bosch BMX160 9-axis IMU, the accelerometer and gyroscope were sampled at 50
128 Hz with a maximum range of ± 8 G and ± 2000 degrees/second, respectively; this data was saved
129 to an SD card on the device. The choice of 50 Hz was to replicate the typical limitations of
130 consumer devices, which sample the IMU at lower sampling rates than research-grade devices
131 due to battery and bandwidth constraints, we also performed a pre-study on 6 participants with
132 sample rates of 10 – 1000 Hz with 50 Hz showing good accuracy on peak force reconstruction.
133 The choice of ± 8 G was informed by an experiment looking at maximum acceleration
134 experienced by the ear-worn IMU during running, this rarely exceeded 4 G, so 8 G was chosen
135 as the range. The ear-worn device has a form factor similar to a hearing aid with a larger part
136 containing the IMU, computational and radio modules behind the ear and an earpiece fitted
137 with a yellow foam eartip (Figure 1.c). Whilst the device reliably sits in the ear, it was secured
138 with an elastic headband for safety (Figure 1.a).

139 After a self-directed warm-up, participants were asked to run at different speeds both
140 on an instrumented treadmill (Bertec, OH, USA, 1000 Hz) and overground. Treadmill
141 running was carried out with no belt incline and included bouts of 4 minutes running,

142 interspersed by at least 2 minutes recovery, at 10 km/h (common to all participants) and 2
143 other self-selected speeds (e.g., 11-12 km/h). In the overground condition, runners looped
144 around the lab for 3 minutes at a self-selected speed and, without targeting, stepped on four
145 900 × 600 mm Kistler force plates (mod 9667A0906, Kistler, Winterthur, Switzerland, 1000
146 Hz) when transitioning in the central part of the room (Figure 1.b). This condition was used
147 to create a higher variance of gait parameters in the dataset. At the start of each recording,
148 participants performed a series of foot stamps to allow the manual synchronisation of force
149 plates and ear-worn sensors by matching the initial series of peaks, to allow matching stance
150 phases from the different data streams.

151 Treadmill GRF was pre-processed with a 15 Hz Butterworth 5th-order low-pass filter,
152 with a forward and backward pass to avoid phase distortion but was kept at the original
153 sampling frequency (1000 Hz) after filtering. This filter was used to eliminate noise from
154 mechanical vibrations of the treadmill belt and structure as the gradient changing model can
155 suffer from vibrations [4]. Overground GRF was pre-processed with a 100 Hz low-pass filter
156 as they were fixed models, the higher sampling rate can assess generalisation of the
157 algorithms. Thresholds of 40 and 20 N were used for treadmill and overground conditions,
158 respectively, to identify individual contacts and the temporal metrics derived thereof (i.e.,
159 cadence, stride time, stance time, flight time).

160 An algorithm was developed to use accelerometer and gyroscope data from both ear-
161 worn devices (left and right ears) to: (1) detect heel strike and toe-off from each gait cycle;
162 (2) segment the IMU data into individual flight and stance periods; (3) calculate spatio-
163 temporal features, such as cadence, stride time, stance time, and flight time; and (4) predict
164 vGRF waveforms and scalar metrics, which included peak values, impulse, and loading rate,
165 as defined by the gradient between the point where the vGRF curve first exceeded 200 N to
166 90% of the impact peak, as used previously in running studies [21]. The ground truth peak

167 force was always taken as the active peak; this was detected by finding the highest force in
168 the stance region which was active peak over the impact peak in every example that was
169 checked.

170 The principle of the segmentation algorithm was finding heel strike and toe-off gait
171 events. Both gait events had corresponding patterns in the head acceleration signals (Figure
172 2). The heel strike was detected from the onset of the impact peak, which was captured in the
173 second derivative of the vertical acceleration signal as the first of two peaks that occurred
174 during the loading phase. To improve the accuracy of the measurement, the left and right
175 earbud channels were summed, which strengthened the trend in the acceleration signal,
176 giving more prominent peaks. The toe-off was detected by first applying a low-pass filter
177 with a 10 Hz cutoff to the acceleration signal, this was then differentiated to give the jerk
178 signal; upon inspection of the jerk signal, an inflection point could be seen that corresponded
179 with the toe-off (Figure 2). This could be detected by looking for a local minimum in the
180 derivative of the jerk signal. These events were combined with a system that checked realistic
181 timing, i.e., a flight phase that was not over 0.5 s or under 5 ms. While not all gait events
182 were correctly detected, no manual edits were made to this process and the reported results
183 are made only from the described algorithm.

184 vGRF estimation used machine learning regression models. First, discrete scalar
185 parameters—peak force, loading rate, and impulse—were estimated with predictions made by
186 the regression model in body weight units (BW), as the training data was normalised by the
187 user's body weight. This was rationalised by the user only needing to input their weight into
188 the system to obtain predictions in Newtons if desired. The scalars were estimated using
189 Gaussian process regression using time and frequency domain features calculated over the
190 segmented IMU data for that stance phase.

191 The scalar measures were then combined with the raw IMU signals to regress the
192 vGRF curve. The model for this sequence-to-sequence regression was a fixed number of
193 boosted tree models, one for each vGRF sample. Each model saw every IMU sample from
194 the stance phase and the estimated scalars to predict a single output point; this was then
195 repeated for each output time point. Finally, the predicted vGRF waveform was post-
196 processed with the same low-pass filter used on the ground truth, i.e., 15 Hz for treadmill
197 data. The number of output time samples must be the same for each stance phase due to the
198 fixed size of the machine learning model; this results in uneven sampling rates as the stance
199 period can vary in length between steps and participants. This length was configurable
200 depending on the granularity of predicted vGRF desired, but we presented results for 100
201 time samples, which corresponded to between 400-500 Hz depending on the exact stance
202 time. This was chosen as it was above the Nyquist criterion for the 15 Hz and 100 Hz low-
203 pass filter cut-off frequencies used on the treadmill and force plate data, respectively, so
204 would still capture all trends in the pre-processed ground truth. The overall information flow
205 described here is shown in Figure 3, and the model presented here was derived from the
206 model developed in [31] used for walking vGRF estimation from earables. Data from the
207 treadmill or force plates is not included here as it was used for validation of the proposed
208 system.

209 The treadmill allowed a large volume (~54,000) of step samples to be collected for
210 model training, whilst the force data from plates with relatively fewer samples (~2,800) was
211 used as ground truth to validate the algorithm in the more common overground running
212 scenario.

213 We compared predicted quantities and ground truth using a selection of accuracy
214 metrics and validation schemes; this allowed for comparison with a greater amount of related
215 works. Scalar quantities were assessed in terms of Mean Absolute Error (MAE), Mean

216 Absolute Percentage Error (MAPE), and Pearson Correlation Coefficient (Corr). A Bland-
217 Altman analysis with Reproducibility Coefficient (RPC) and 95% Limits of Agreement
218 (LOA) was also presented. Time series estimation was analysed through Root Mean Square
219 Error (RMSE), Normalised Root Mean Square Error (NRMSE), normalised as a percentage
220 to the ground truth value on a sample-by-sample basis, and the Pearson Correlation
221 Coefficient of each point.

222 The regression evaluation used three validation schemes; these schemes were only
223 relevant for the kinetic scalar and vGRF curve results, as temporal parameters were estimated
224 with signal processing techniques requiring no training data. The first scheme was Unseen
225 4:1, using a 4:1 train:test data split ratio. The test set was comprised of only unseen users; this
226 ratio had 24 users in the training set and 6 users in the test set. The second was Leave One
227 Subject Out (LOSO) validation, which trained on 29 users whilst leaving out a single user.
228 Finally, we also presented a Mixed (4:1) validation scheme, which used a mixed batch of data
229 in a 4:1 train:test ratio. This did not repeat gait cycles, but users could be repeated in the test
230 and train sets. This was included to allow comparison with works that did the same. The
231 mixed and unseen were validated on 5 randomly sampled 4:1 sets and the LOSO on all 30
232 possible combinations. For the overground evaluation, training data was in the Unseen 4:1
233 ratio, where training data was taken from the 24 training participants on both the treadmill
234 and force plates, and the testing data was from the 6 unseen participants' force plate data.

235

236

Results

237 Errors consistently lower than 20 ms were found for temporal measures between the
238 treadmill and ear-worn device, with a high correlation of predicted temporal gait metrics
239 compared to the treadmill data, providing an IMU segmentation that tracked the stance phase
240 for the kinetic parameter stage (Table 1). A Bland-Altman analysis showed low RPC for stride

241 time with higher percentage RPC for stance and flight times, indicating that toe-off detection
242 was less accurate than heel strike detection. The Bland-Altman analysis also showed the 95%
243 LOA had a similar trend per gait metric as seen for the RPC. A bias in stance and flight times
244 of +0.01 and -0.01, respectively, was observed (Figure 4).

245 The kinetic scalar gait parameters showed MAPEs below 10% for peak force and
246 impulse and below 20% for loading rate between ground truth and predictions (Table 2). The
247 correlation was higher for the 4:1 unseen group and lower for the LOSO group. The RPC was
248 low for both peak force and impulse but much higher for loading rate at 60% (Figure 4).
249 Similarly, the LOA followed the same trend across the kinetic metrics (Figure 4).

250 vGRF estimation in the mixed evaluation scenario had an NRMSE of 7.6%, followed
251 by the more realistic unseen scenario with an NRMSE of 11.1% and LOSO with 13.1% (Table
252 2). Different examples for individual vGRF curves showed differences in the tracking accuracy
253 for different participants given for the lowest (Figure 5a), average (Figure 5b and c), and
254 highest (Figure 5d) RMSE participants relative to the dataset. For the two participants with
255 average RMSE, it could be seen that one example captured (Figure 5b) the impact peak but had
256 poor tracking during and after the active peak, whilst the other (Figure 5c) missed the impact
257 peak but had good tracking around and after the active peak. The comparison between the
258 lowest and highest RMSE participants both showed a forefoot strike example where tracking
259 was relatively good for the lowest (Figure 5a) or poor for the highest (Figure 5d).

260 The per-user error across the participants for temporal parameters varied between 3%-
261 8% (Figure 6a). For kinetic scalars, most participants had a constant MAPE around 5% in the
262 LOSO validation, but a few participants had much higher values near 15% (Figure 6b), the
263 higher error was dominated by the loading rate error. The vGRF showed a similar pattern to
264 the kinetic scalar with variations in NRMSE of 8%–19% across the participants in the LOSO
265 validation (Figure 6c).

266 In the overground experiments, the errors increased on all predicted gait parameters
 267 compared to the treadmill scenario; this was a small increase for temporal parameters of below
 268 1%, but for kinetic scalars and vGRF estimation this was up to 4% higher. This might have
 269 been caused by the higher variance in running style in the untargeted overground experiments
 270 compared to the training data taken from the more controlled treadmill experiments or could
 271 be due to a relative lack of model training samples with only 2800 overground steps compared
 272 to 54000 treadmill steps.

273

274 **Table 1:** Results for temporal gait parameters evaluated for all 30 participants on the
 275 treadmill data, totalling around 54000 step samples.

| Metric | Cadence | Stride Time | Stance Time | Flight Time |
|-------------|--------------|-------------|-------------|-------------|
| MAE | 3.5 step/min | 8.2 ms | 11.9 ms | 11.9 ms |
| MAPE | 2.2% | 1.1% | 4.49% | 11.1% |
| Correlation | 0.872 | 0.960 | 0.883 | 0.885 |

276

277 **Table 2:** Results for kinetic scalar parameters and vGRF under the three different validation
 278 conditions, units and evaluation metrics are specified in the second row. Evaluated for all 30
 279 participants on the treadmill data, totalling around 54000 step samples.

| Validation Scheme | Peak Force | | | Loading Rate | | | Impulse | | | vGRF | |
|-------------------|------------|-------|-------|--------------|-------|-------|-------------|-------|-------|------------|------------|
| | MAE BW | MAPE% | CORR | MAE BW/s | MAPE% | CORR | MAE BW.s | MAPE% | CORR | RMSE BW | NRMSE % |
| Unseen 4:1 | 0.143 | 6.03% | 0.890 | 0.028 | 18% | 0.693 | 0.015 | 3.8% | 0.639 | 0.154 | 11.14 |

| | | | | | | | | | | | |
|-----------|-------|-------|-------|-------|-----|-------|-------|------|-------|-------|-------|
| LOSO 29:1 | 0.145 | 6.38% | 0.417 | 0.032 | 22% | 0.323 | 0.016 | 4.2% | 0.324 | 0.182 | 13.09 |
| Mixed 4:1 | 0.100 | 4.10% | 0.901 | 0.025 | 14% | 0.774 | 0.013 | 3.5% | 0.716 | 0.112 | 7.56 |

280

281

Discussion

282

283

284

285

286

287

288

289

In this study, we aimed to develop and test a system that harnessed the potential of inertial sensors embedded in consumer-oriented earbuds and fed their data into a predictive model that estimated key biomechanical quantities for running assessment. From the assessment we carried out through treadmill and overground running on 30 participants, the system demonstrated an overall accuracy of 4.8% on temporal metrics and 11.1% on vGRF curve estimation, which was comparable to what was achieved by purpose-made gait assessment systems, whilst offering advantages in terms of being deployed on a comfortable, commonly owned device that could also be used for entertainment.

290

291

292

293

The presented algorithm was lightweight, with signal processing and machine learning models shown to run in real time on an iPhone device [31]. Additionally, the model used for kinetic scalars in this study could have been simplified even further, as the Gaussian Process model had a longer inference period than techniques such as support vector regression.

294

295

296

297

298

299

300

301

In this study, we used a relatively low sampling rate of 50 Hz compared to many studies that conducted running gait assessment with inertial sensors, i.e., 1000 Hz [11] and 2000 Hz [1]. This was done to demonstrate the performance on typical consumer devices (i.e., Apple AirPods Pro (Apple Inc., Cupertino, CA, USA) 25 Hz) or modified Samsung Galaxy Buds [15] that would be used in real scenarios with the algorithms developed. Furthermore, we believe that the integration of running metrics into devices such as heart rate straps (Garmin Ltd., KS, USA) showcases a prior viable route for running gait analysis integration into non-purpose made device form factors.

302

303

Related works used purpose-made or research devices that might have required attachment to shoes or the torso, which could have represented additional cost to potential users

304 compared to earables that were commonly owned and served additional purposes. In terms of
305 accuracy of these systems for temporal parameters, shoe-mounted IMU methods had achieved
306 MAEs of 8 ms with signal processing [6] and 15 ms with machine learning [12] compared to
307 our MAE of 12 ms. For a sacrum-mounted IMU using machine learning, MAPEs of 9.3% and
308 3.6% [25] were obtained for flight and stance times compared to MAPEs of 11.1% and 4.5%
309 for our system. Both comparisons showed that an earable device obtained comparable temporal
310 metric accuracy against devices that would have been purpose-made for gait assessment.

311 For vGRF curve prediction, we reported an NRMSE of 11%. For related works using
312 IMUs on the sacrum and shoes, vGRF curve prediction was reported as NRMSEs of 6.5% [1]
313 and 6.1–9.1% [11], and insole-based systems reported between 0.8 and 8.8% [4], all using
314 machine learning models. For kinetic scalars, a study with a sacrum-mounted device tested the
315 peak force, loading rate, and impulse [1], obtaining MAPEs of 8.8%, 27.6%, and 6.4%,
316 respectively, compared to our results of 6.0%, 18%, and 3.8%. This showed that for vGRF
317 information, the earable device was also close to the purpose-made devices despite using more
318 lightweight techniques and having a more complex dynamic relationship to capture due to the
319 neck and head. It was likely that through a combination of more powerful modelling
320 approaches, such as an LSTM [1, 4], and a larger dataset size, the results reported here could
321 have been improved upon. However, system constraints on power, computational power, and
322 latency would have had to be considered based upon the application and processing devices
323 available if a larger model were to have been used.

324 A bias could be seen in flight and stance time Bland-Altman plots (Figure 4), which
325 might have been caused by the threshold used to segment the treadmill ground truth. The
326 threshold could lead to an underestimate of the stance time, which would explain the
327 overestimate in the earable predictions. This could be seen visually in an example in Figure 2
328 as well as in the trend in Bland-Altman plots (Figure 4), so it was likely that the temporal metric

329 performance was better than reported due to the described error in the treadmill timings. This
330 could be investigated in future work using other validation systems such as motion capture or
331 hand labelling of the force plate data.

332 The reported error for temporal gait metrics was close to the best case for a sampling
333 rate of 50 Hz. This "best case" could be estimated by assuming exact gait events were randomly
334 distributed uniformly within the sensor sampling interval. Given that each interval was 20 ms
335 apart and that the algorithm always predicted the closest sample, the highest and lowest errors
336 were 10 ms and 0 ms, with an average error of 5 ms. Thus, on average, the MAE could be at a
337 minimum of 5 ms using a 50 Hz sensor with no interpolation or upsampling, assuming a perfect
338 gait event detection algorithm. Given that 5 ms was the best achievable result for gait event
339 detection with a 50 Hz sampling rate, the reported MAEs (Table 1) showed that the earable
340 gait event detection algorithm was close to this value, demonstrating accurate detection of gait
341 events.

342 To assess the participants who had lower accuracy in the kinetic scalar estimation
343 (Figure 6), it was found that participants 6 and 11 had the largest peak force values in the
344 dataset, over 3 BW. When the model was trained in the LOSO setting, it only saw a small
345 amount of data of this magnitude and was therefore less likely to make accurate predictions.
346 Participants 18 and 27 had a similar case but with the smallest peak forces, typically below 2
347 BW. The increase in peak force also affected the loading rate and impulse values. For the vGRF
348 prediction, the same participants had higher errors compared to the kinetic scalars, where the
349 same reasoning applied. Scaling up to more participants might have improved the performance
350 on users who were outliers in the current participant population. Another cause of cross
351 participant variation may be caused by decoupling of a device from the head. In most cases the
352 left and right earable IMU signals were similar in morphology. However, in a few experiments
353 one device showed more high frequency energy which may indicate a looser coupling with the

354 head in those experiments. This may result in lower accuracy predictions as there is high noise
355 content in the signal.

356 In the kinetic scalar estimation, the loading rate had the worst RPC and highest MAPE,
357 showing it was the most poorly estimated parameter. This could have been because the features
358 used were less relevant to predicting the loading rate compared to the other parameters, as the
359 features were calculated over the whole stance phase rather than just the loading period. The
360 correlations were higher in the unseen validation compared to the LOSO validation across all
361 three estimated parameters (Table 2). This could have implied that the magnitude of the
362 parameters was estimated well, but the method was less sensitive to the trends within a single
363 experiment or user.

364 A limitation of this study was head motions, such as rotating the head to talk to a friend;
365 these would register high accelerometer values on the earables that were not related to gait,
366 potentially affecting gait event detection or regression predictions. Whilst this was not tested
367 for in this study, participants were not instructed to keep their head still, so the reported results
368 included any errors incurred through head motions made during the data collection process. In
369 other work, this was mitigated by the gyroscope signal, which was large in magnitude during
370 head rotations compared to gait due to the orders of magnitude difference in radius of rotation.
371 This allowed easy detection of head motion to remove these segments of the data entirely [31];
372 however, a more advanced compensation scheme could have been developed using the
373 gyroscope to remove the head motion-related acceleration components.

374 A further limitation of this study is that the footstrike type for the participants was not
375 systematically recorded. However, we believe that the model has learnt to be agnostic to
376 footstrike type given the correct vGRF morphologies shown in Figure 5. There are also prior
377 studies that show IMU data can be used to classify footstrike type with high accuracy, e.g. [30],

378 which gives further confidence that a model can learn important information about footstrike
379 from IMU data.

380 Future development on this work could explore estimation of further biomechanical
381 parameters in running from the head, examples include tibial bone force [23] and ground
382 reaction moments [18], both of which have been estimated with wearable devices. Another
383 future direction could incorporate the algorithms developed here onto fully mobile devices such
384 as the earbuds themselves or an earbud – phone pairing to test the performance in the field.

385 **Conclusion**

386 Overall, we demonstrated for the first time the promise of using consumer ear-worn
387 wearables to perform gait timing and loading analysis whilst running with algorithms that are
388 lightweight enough to operate on a mobile phone and possibly the earbuds themselves with
389 further development. We presented algorithms to estimate temporal gait metrics, which were
390 then used to segment and estimate kinetic parameters and the vGRF curve, showing
391 comparable accuracy to purpose-made gait assessment devices that are already popular with
392 consumers. This presents a valuable tool for a range of parties, from amateur runners requiring
393 fewer devices to track key running metrics, to coaches for continuously monitoring
394 performance and elite athletes for real-time feedback on running gait without distractions from
395 screens. This work opens up future research directions on long-term monitoring of running gait
396 to enable research to assess causal relationships with performance and injuries, as well as for
397 tracking athlete rehabilitation and mobile system-based challenges on optimising the system
398 performance for earable-based running gait assessment.

399
400
401
402
403
404
405
406

Acknowledgements

This work was supported by EPSRC grants EP/Z53447X/1 and EP/S023046/1 for the EPSRC CDT in Sensor Technologies and Applications as well as EVIDEN/New Atos Life Sciences Centre of Excellence.

References

- [1] Alcantara RS, Edwards WB, Millet GY, Grabowski AM. Predicting continuous ground reaction forces from accelerometers during uphill and downhill running: a recurrent neural network solution. *PeerJ*. 2022;10:e12752. doi:10.7717/peerj.12752
- [2] Atallah L, Wiik A, Jones GG, et al. Validation of an ear-worn sensor for gait monitoring using a force-plate instrumented treadmill. *Gait & Posture*. 2012;35(4):674-676. doi:10.1016/j.gaitpost.2011.11.021
- [3] Bobbert, M. F., Schamhardt, H. C., & Nigg, B. M. (1991). Calculation of vertical ground reaction force estimates during running from positional data. *Journal of biomechanics*, 24(12), 1095-1105.
- [4] Carter J, Chen X, Cazzola D, Trewartha G, Preatoni E. Consumer-priced wearable sensors combined with deep learning can be used to accurately predict ground reaction forces during various treadmill running conditions. *PeerJ*. 2024;12:e17896. doi:10.7717/peerj.17896
- [5] Ceysens L, Vanelderden R, Barton C, Malliaras P, Dingenen B. Biomechanical Risk Factors Associated with Running-Related Injuries: A Systematic Review. *Sports Med*. 2019;49(7):1095-1115. doi:10.1007/s40279-019-01110-z
- [6] Chew DK, Ngoh KJH, Gouwanda D, Gopalai AA. Estimating running spatial and temporal parameters using an inertial sensor. *Sports Eng*. 2018;21(2):115-122. doi:10.1007/s12283-017-0255-9
- [7] Clark, K. P., Ryan, L. J., & Weyand, P. G. (2017). A general relationship links gait mechanics and running ground reaction forces. *Journal of Experimental Biology*, 220(2), 247-258.
- [8] Clermont CA, Duffett-Leger L, Hettinga BA, Ferber R. Runners' Perspectives on 'Smart' Wearable Technology and Its Use for Preventing Injury. *International Journal of Human-Computer Interaction*. 2020;36(1):31-40. doi:10.1080/10447318.2019.1597575
- [9] Derrick, T. R., Caldwell, G. E., & Hamill, J. (2000). Modeling the stiffness characteristics of the human body while running with various stride lengths. *Journal of Applied Biomechanics*, 16(1), 36-51.
- [10] Diao Y, Ma Y, Xu D, Chen W, Wang Y. A novel gait parameter estimation method for healthy adults and postoperative patients with an ear-worn sensor. *Physiol Meas*. 2020;41(5):05NT01. doi:10.1088/1361-6579/ab87b5
- [11] Dorschky E, Nitschke M, Martindale CF, van den Bogert AJ, Koelewijn AD, Eskofier BM. CNN-Based Estimation of Sagittal Plane Walking and Running Biomechanics From

- 456 Measured and Simulated Inertial Sensor Data. *Front Bioeng Biotechnol.* 2020;8.
457 doi:10.3389/fbioe.2020.00604
458
- 459 [12] Falbriard M, Meyer F, Mariani B, Millet GP, Aminian K. Accurate Estimation of
460 Running Temporal Parameters Using Foot-Worn Inertial Sensors. *Front Physiol.* 2018;9.
461 doi:10.3389/fphys.2018.00610
462
- 463 [13] Globally, how many people practice running (as a sport), and what is the global market
464 size for this sport? Wonder. Accessed June 7, 2025. [https://askwonder.com/research/globally-](https://askwonder.com/research/globally-people-practice-running-as-sport-global-market-size-sport-dba00dqv)
465 [people-practice-running-as-sport-global-market-size-sport-dba00dqv](https://askwonder.com/research/globally-people-practice-running-as-sport-global-market-size-sport-dba00dqv)
466
- 467 [14] How often do you run in comparison to other Runner's World readers? And how does
468 your "easy run" pace compare? *Runner's World.* September 20, 2023. Accessed May 29,
469 2025. [https://www.runnersworld.com/uk/news/a45036050/runners-world-running-survey-](https://www.runnersworld.com/uk/news/a45036050/runners-world-running-survey-2023/)
470 [2023/](https://www.runnersworld.com/uk/news/a45036050/runners-world-running-survey-2023/)
471
- 472 [15] Islam, Md Saiful, et al. "BallistoBud: Heart Rate Variability Monitoring using Earbud
473 Accelerometry for Stress Assessment." *Proceedings of the 2025 CHI Conference on Human*
474 *Factors in Computing Systems.* 2025.
475
- 476 [16] Jarchi D, Wong C, Kwasnicki RM, Heller B, Tew GA, Yang GZ. Gait Parameter
477 Estimation From a Miniaturized Ear-Worn Sensor Using Singular Spectrum Analysis and
478 Longest Common Subsequence. *IEEE Transactions on Biomedical Engineering.*
479 2014;61(4):1261-1273. doi:10.1109/TBME.2014.2299772
480
- 481 [17] Jiang X, Napier C, Hannigan B, Eng JJ, Menon C. Estimating Vertical Ground Reaction
482 Force during Walking Using a Single Inertial Sensor. *Sensors.* 2020;20(15):4345.
483 doi:10.3390/s20154345
484
- 485 [18] Johnson, W. R., Mian, A., Robinson, M. A., Verheul, J., Lloyd, D. G., & Alderson, J. A.
486 (2020). Multidimensional ground reaction forces and moments from wearable sensor
487 accelerations via deep learning. *IEEE Transactions on Biomedical Engineering,* 68(1), 289-
488 297.
489
- 490 [19] Kluge F, Brand YE, Micó-Amigo ME, et al. Real-World Gait Detection Using a Wrist-
491 Worn Inertial Sensor: Validation Study. *JMIR Formative Research.* 2024;8(1):e50035.
492 doi:10.2196/50035
493
- 494 [20] LeBlanc B, Hernandez EM, McGinnis RS, Gurchiek RD. Continuous Estimation of
495 Ground Reaction Force During Long Distance Running Within a Fatigue Monitoring
496 Framework: A Kalman Filter-Based Model-Data Fusion Approach. *Journal of Biomechanics.*
497 2021;115:110130. doi:10.1016/j.jbiomech.2020.110130
498
- 499 [21] Lieberman DE, Venkadesan M, Werbel WA, et al. Foot strike patterns and collision
500 forces in habitually barefoot versus shod runners. *Nature.* 2010;463(7280):531-535.
501 doi:10.1038/nature08723
502
- 503 [22] Matijevich, E. S., Branscombe, L. M., Scott, L. R., & Zelik, K. E. (2019). Ground
504 reaction force metrics are not strongly correlated with tibial bone load when running across

505 speeds and slopes: Implications for science, sport and wearable tech. PloS one, 14(1),
506 e0210000.

507

508 [23] Matijevich, Emily S., et al. "Combining wearable sensor signals, machine learning and
509 biomechanics to estimate tibial bone force and damage during running." *Human movement*
510 *science* 74 (2020): 102690.

511

512 [24] Nedergaard, N. J., Verheul, J., Drust, B., EtcHELLS, T., Lisboa, P., Robinson, M. A., &
513 Vanrenterghem, J. (2018). The feasibility of predicting ground reaction forces during running
514 from a trunk accelerometry driven mass-spring-damper model. *PeerJ*, 6, e6105.

515

516 [25] Patoz A, Lussiana ,Thibault, Breine ,Bastiaan, Gindre ,Cyrille, and Malatesta D.
517 Comparison of different machine learning models to enhance sacral acceleration-based
518 estimations of running stride temporal variables and peak vertical ground reaction force.
519 *Sports Biomechanics*. 0(0):1-17. doi:10.1080/14763141.2022.2159870

520

521 [26] Preatoni E, Bergamini E, Fantozzi S, et al. The Use of Wearable Sensors for Preventing,
522 Assessing, and Informing Recovery from Sport-Related Musculoskeletal Injuries: A
523 Systematic Scoping Review. *Sensors*. 2022;22(9):3225. doi:10.3390/s22093225

524

525 [27] Provot T, Choupani S, Bourgain M, Valdes-Tamayo L, Chadefaux D. Using Wearable
526 Accelerometers to Develop a Vertical Ground Reaction Force Prediction Model during
527 Running: A Sensitivity Study. *Vibration*. 2023;6(3):680-694. doi:10.3390/vibration6030042

528

529 [28] Röddiger T, Stuchbury-Wass J, Ciliberto M, Lepold P, Beigl M. OpenEarable 1.4: Dual
530 Microphones Earpiece to Capture In-Ear and Outer-Ear Audio Signals. In: Companion of the
531 2024 on ACM International Joint Conference on Pervasive and Ubiquitous Computing.
532 UbiComp '24. Association for Computing Machinery; 2024:930-933.
533 doi:10.1145/3675094.3678483

534

535 [29] Seifer AK, Dorschky E, Küderle A, Moradi H, Hannemann R, Eskofier BM. EarGait:
536 Estimation of Temporal Gait Parameters from Hearing Aid Integrated Inertial Sensors.
537 *Sensors*. 2023;23(14):6565. doi:10.3390/s23146565

538

539 [30] Shiang, T. Y., Hsieh, T. Y., Lee, Y. S., Wu, C. C., Yu, M. C., Mei, C. H., & Tai, I. H.
540 (2016). Determine the foot strike pattern using inertial sensors. *Journal of Sensors*, 2016(1),
541 4759626.

542

543 [31] Stuchbury-Wass J, Liu Y, Butkow KJ, et al. WalkEar: Holistic Gait Monitoring using
544 Earables. In: 2025 IEEE International Conference on Pervasive Computing and
545 Communications (PerCom). 2025:200-209. doi:

546

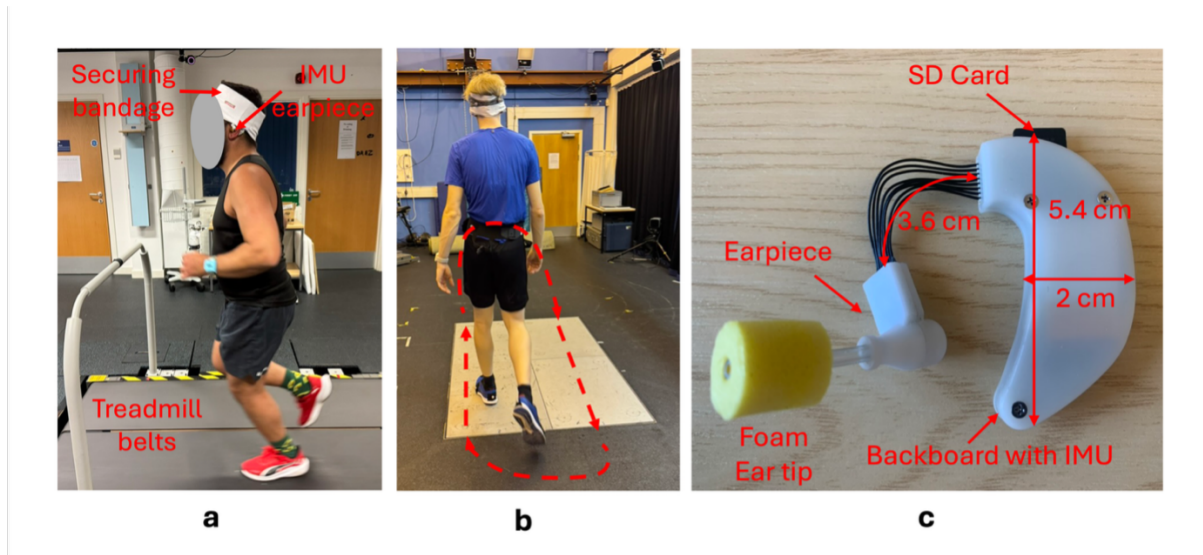
547 [32] van der Worp H, Vrieling JW, Bredeweg SW. Do runners who suffer injuries have
548 higher vertical ground reaction forces than those who remain injury-free? A systematic
549 review and meta-analysis. *Br J Sports Med*. 2016;50(8):450-457. doi:10.1136/bjsports-2015-
550 094924

551

552 [33] Van Hooren B, Goudsmit J, Restrepo J, Vos S. Real-time feedback by wearables in
553 running: Current approaches, challenges and suggestions for improvements. *Journal of Sports*
554 *Sciences*. 2020;38(2):214-230. doi:10.1080/02640414.2019.1690960

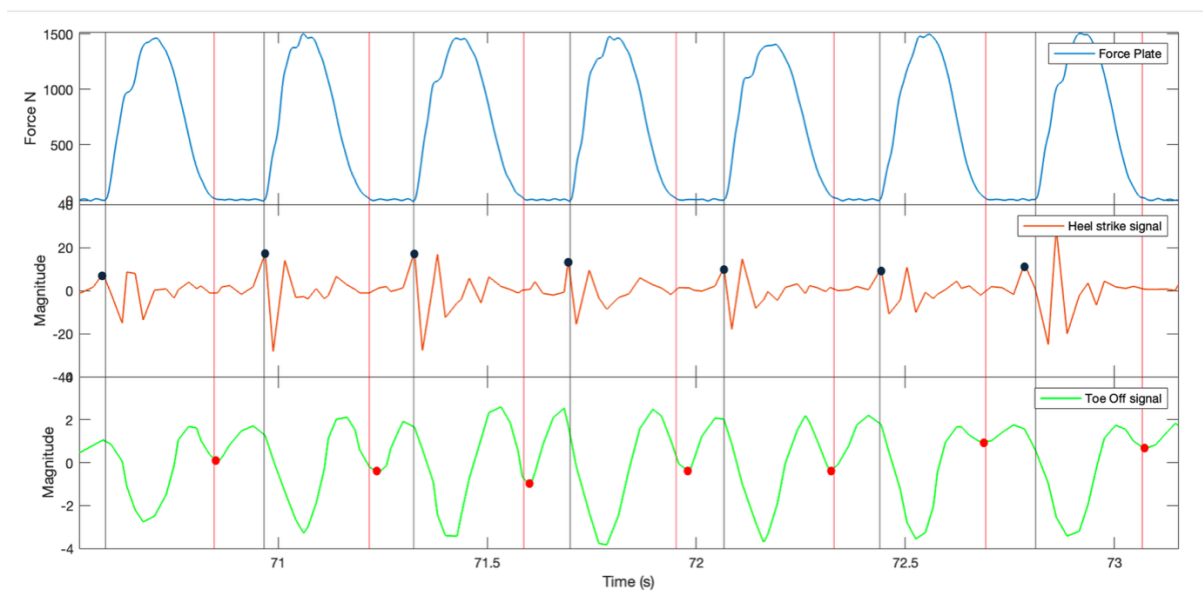
555 [34] Zhu Y, Xia D, Zhang H. Using Wearable Sensors to Estimate Vertical Ground Reaction
556 Force Based on a Transformer. Applied Sciences. 2023;13(4):2136.
557 doi:10.3390/app13042136
558
559

Figure Captions



560

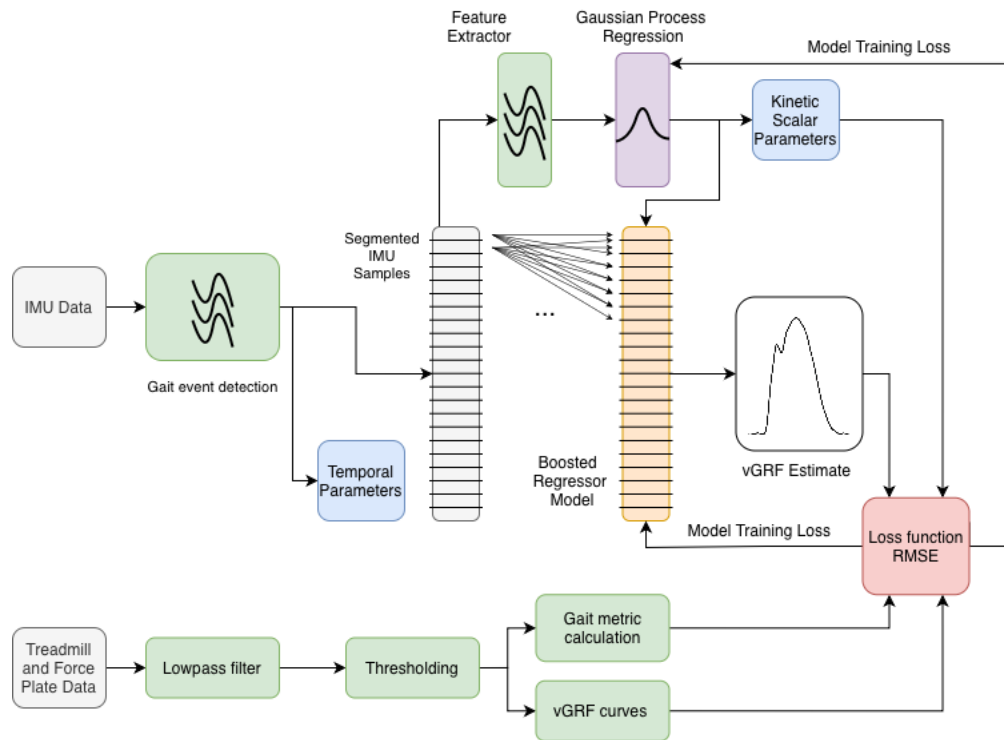
561 **Figure 1** – Experimental setup showing (a) a participant running on a single instrumented
562 treadmill whilst wearing the OpenEarable IMU earpiece secured with a bandage. (b) a
563 participant walking over the footplates with a rough travel path annotated. (c) the
564 OpenEarable 1.4 device with key dimensions annotated.



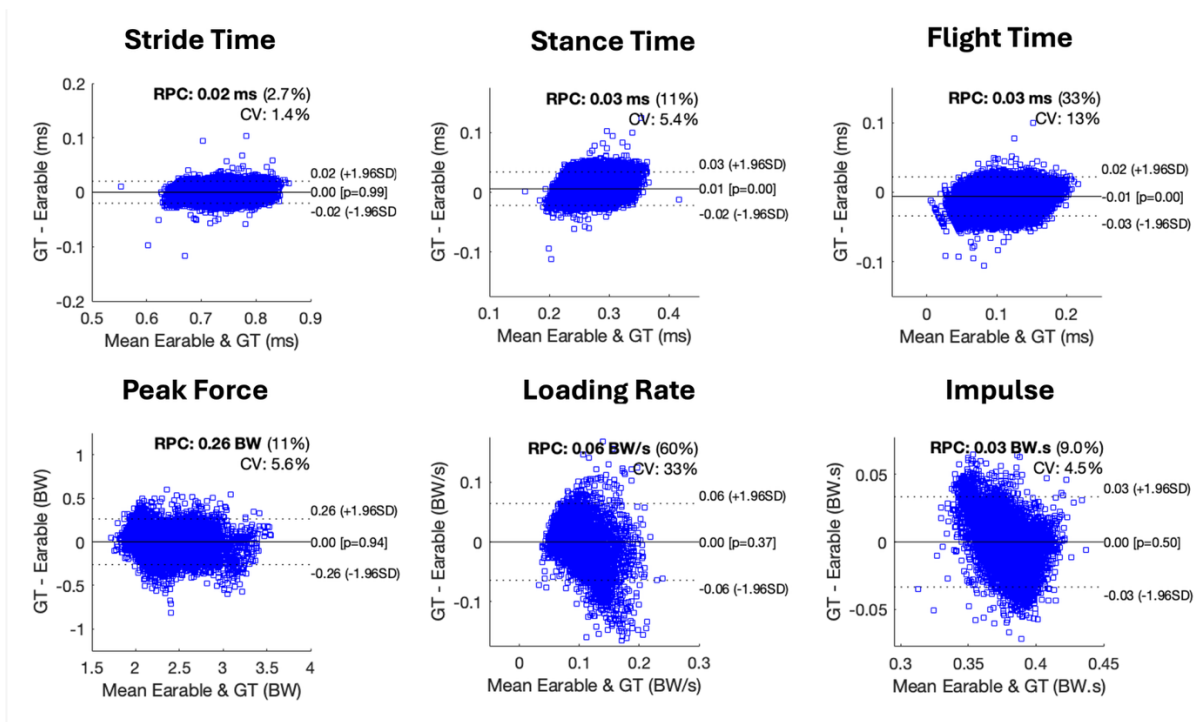
565

566 **Figure 2** – Example of the head accelerometer gait event detection algorithm with a
567 comparison to the treadmill data (top). Heel strikes are shown in a black line as ground truth

568 and a black dot as the estimation, both can be seen with the IMU second derivative signal
 569 (middle). The toe-off is shown as a red line for ground truth and a red dot for estimation
 570 results, both can be seen in the filtered IMU second derivative signal (bottom).



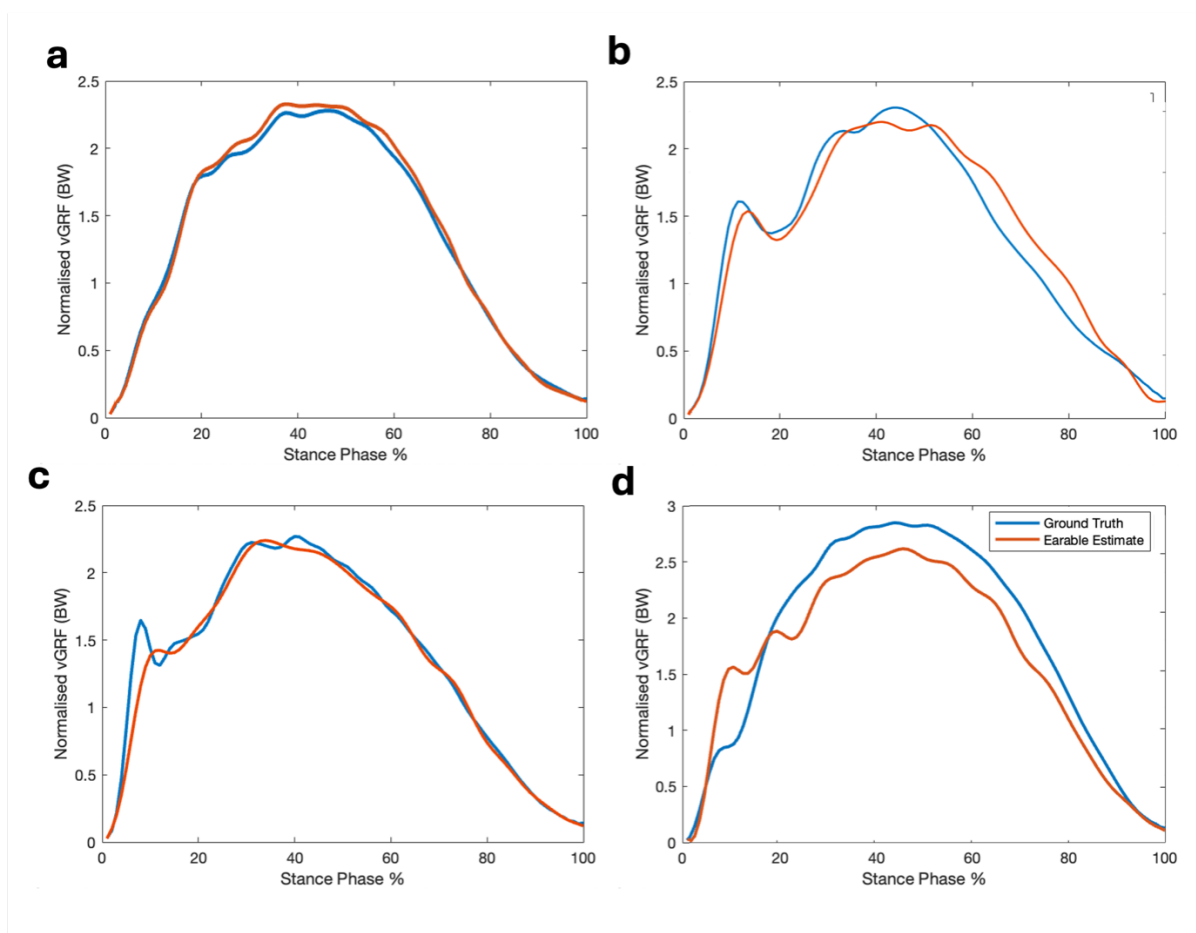
571
 572 **Figure 3** – Block diagram showing the flow of information from the ear-worn IMU to predict
 573 the gait parameters and reconstruct the vGRF curve. Each of the three kinetic scalars is
 574 regressed using the segmented IMU data then fed into the boosted regressor models which
 575 use both the kinetic scalars and IMU data as an input to regress the vGRF curve. The output
 576 is 100 time samples over the stance period making up the vGRF estimate. The ground truth
 577 data from the treadmill and force plates are shown with preprocessing steps as well as input
 578 to a loss function to train the Gaussian process and vGRF regression models.



579

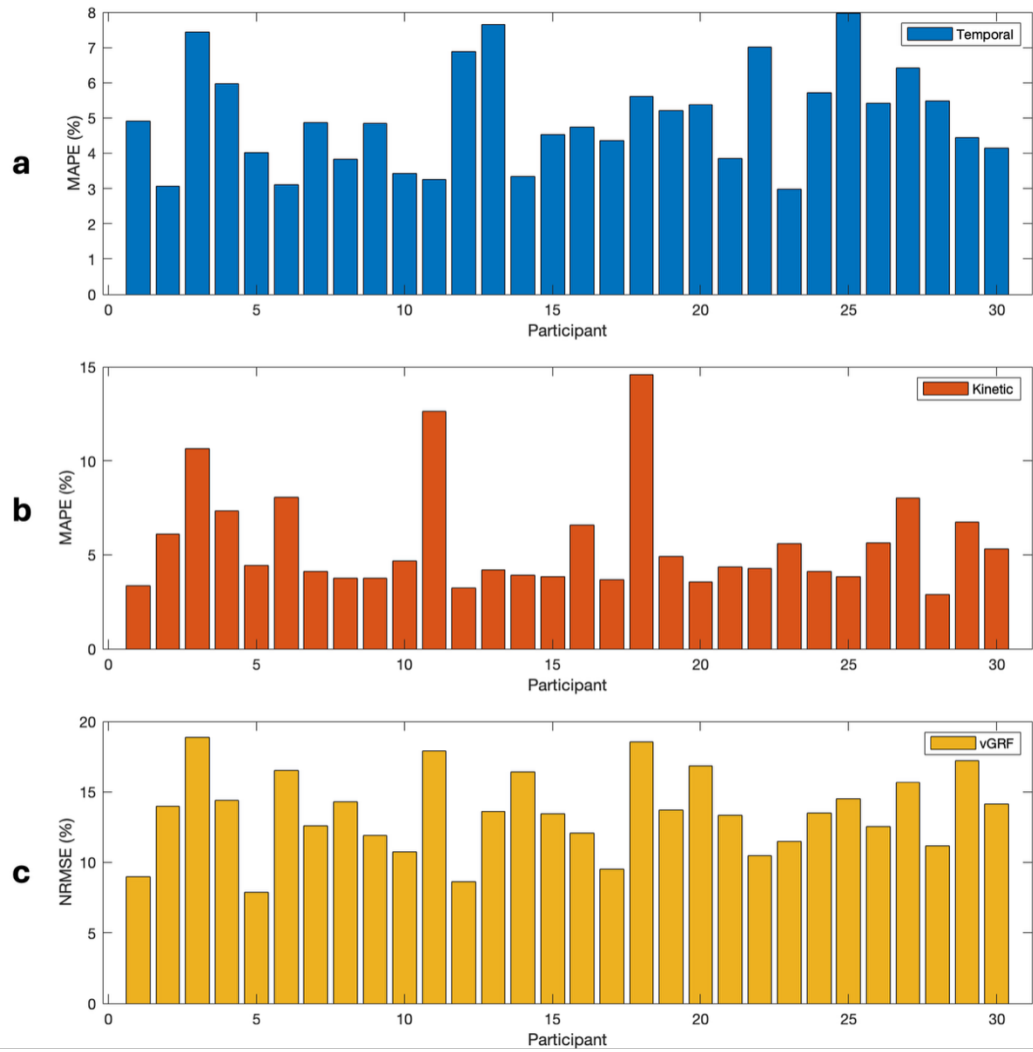
580 **Figure 4** – Six Bland-Altman diagrams of temporal (top) and kinetic (bottom) gait
 581 parameters. Showing ± 1.96 (95%) Limits of Agreement (LOA) and the mean difference with
 582 a p value for a t-test to indicate significance. The diagrams also show Reproducibility
 583 Coefficient (RPC) and its percentage value of the quantity as well as the Coefficient of
 584 Variation (CV), the standard deviation of mean values is shown. The data shown includes all
 585 30 participants' treadmill data amounting to around 54000 samples for temporal parameters
 586 and 10800 samples (one of 5 folds with 6 unseen participants) for kinetic parameters.

587



588

589 **Figure 5** – Four example vGRF curve predictions (orange) with treadmill ground truth shown
 590 (blue). Showing a closely tracked forefoot strike from a low error participant who was an
 591 experienced runner (a). A correctly predicted impact peak but poor tracking of the peak and
 592 unloading phase from an average error participant (b). A missed impact peak in a prediction
 593 from an average error participant (c). A poor tracking example from the highest error
 594 participant (d).



595

596 **Figure 6** – Per Participant error bar chart showing MAPE for temporal (a), kinetic scalars (b)

597 and NRMSE for vGRF curves (c).